Delft University of Technology

Document Version
Final published version

Licence
CC BY

Citation (APA)
Lambarska, A., Hanefeld, U., van der Weel, L., Strampraad, M., Maresz, K., Pudło, W., & Szymańska, K. (2026). Process intensification in chiral cyanohydrin synthesis: From biocatalyst engineering to bioreactor design. *Chemical Engineering Research and Design*, *231*, 733-743. https://doi.org/10.1016/j.cherd.2026.06.050

Important note
To cite this publication, please use the final published version (if applicable).
Please check the document version above.

Copyright
In case the licence states “Dutch Copyright Act (Article 25fa)”, this publication was made available Green Open Access via the TU Delft Institutional Repository pursuant to Dutch Copyright Act (Article 25fa, the Taverne amendment). This provision does not affect copyright ownership.
Unless copyright is transferred by contract or statute, it remains with the copyright holder.

Sharing and reuse
Other than for strictly personal use, it is not permitted to download, forward or distribute the text or part of it, without the consent of the author(s) and/or copyright holder(s), unless the work is under an open content license such as Creative Commons.

Takedown policy
Please contact us and provide details if you believe this document breaches copyrights.
We will remove access to the work immediately and investigate your claim.

This work is downloaded from Delft University of Technology.

Chemical Engineering Research and Design 231 (2026) 733–743

Contents lists available at ScienceDirect

Chemical Engineering Research and Design

journal homepage: www.elsevier.com/locate/cherd

Process intensification in chiral cyanohydrin synthesis: From biocatalyst engineering to bioreactor design

Aleksandra Lambarska [a,b], Ulf Hanefeld [b], Laura van der Weel [b], Marc Strampraad [b], Katarzyna Maresz [c], Wojciech Pudło [a], Katarzyna Szymańska [a,*]

[a] Department of Chemical Engineering and Process Design, Silesian University of Technology, Ks. M. Strzody 7, Gliwice 44-100, Poland
[b] Biokatalyse, Afdeling Biotechnologie, Technische Universiteit Delft, Van der Maasweg 9, Delft 2629Hz, the Netherlands
[c] Institute of Chemical Engineering, Polish Academy of Sciences, Bałtycka 5, Gliwice 44-100, Poland

ARTICLE INFO

Keywords:
Biocatalyst engineering
Bioreactor engineering
Bifunctionalisation
Chiral cyanohydrins
Continuous flow processes
Enzyme immobilisation
Structured monolithic microreactors

ABSTRACT

Enzymes are key green catalysts in the selective synthesis of high-value compounds. Their activity and stability depend not only on the enzyme's structure, but can also be modified by immobilisation method and type of reactors applied. In this context, carriers are often essential for the effective use of enzymes, and the chemical nature of the carrier surface can significantly impact the enzymes and reaction components. *Gt*HNL-A40H/V42T/Q110H (*Gt*HNL-3V) from *Granulicella tundricola* was therefore immobilised on silica carriers functionalised with amino, epoxy and *n*-octyl groups, including bifunctional carriers. Carriers with amino or epoxy groups enable the covalent binding of enzymes. Silica carriers with *n*-octyl groups are characterised by hydrophobic interactions, which, given the structure of *Gt*HNL-3V, can stabilise the enzyme. The process was carried out in two types of reactors: batch and flow. It has been demonstrated that, depending on the type of reactor, bifunctionalised carriers can stabilise the enzyme or facilitate product release, resulting in higher reaction rates compared to monofunctional supports. It was also found that increasing protein loading improved enantioselectivity more effectively than lowering reaction temperature. In continuous flow, reaction volume was halved, and time was reduced from 1 h to 6 min, while minimising potential hydrogen cyanide release and reducing solvent consumption, thereby enhancing process safety and sustainability. These findings highlight the potential of bifunctional carriers for the efficient synthesis of chiral cyanohydrins, with broader applicability to other enzymatic transformations, including biphasic systems.

1. Introduction

Modern science and industry strive to synthetise chemical compounds according to the principles of green chemistry (Sheldon and Brady, 2022; Ganesh et al., 2021; Woodley, 2020). This includes reducing the number of synthesis steps, many of which have economical and environmental costs associated with the multi-step isolation and purification of individual intermediates, as well as the consumption of significant amounts of solvents or energy (Lozano and García-Verdugo, 2023; Newman and Jensen, 2013). In this context, the use of enzymes as catalysts is an expedient solution to significantly reduce the number of steps (Bracco et al., 2016; Sheldon and Pereira, 2017; Woodley, 2025). Of particular interest is the biocatalytic formation of chiral compounds, which are precursors in the broader pharmaceutical, cosmetic and food chemistry sectors (Hanefeld et al., 2022; Guan et al., 2023). Examples include chiral cyanohydrins, as precursors in the synthesis of α-hydroxy aldehydes and ketones, β-amino alcohols, etc (Guan et al., 2023; Torrelo et al., 2014; Griengl et al., 1997). These compounds can also be synthesised using either *(R)*- or *(S)*-selective hydroxynitrile lyases (HNLs) (Dadashipour and Asano, 2011; Padhi, 2017). The use of these enzymes allows not only high substrate conversions to be achieved, but also an enantiomeric excess close to 100%. HNLs are applied in the chemical and biotechnology industries due to their ability to catalyse C-C bond forming reactions (Jangir and Padhi, 2019; Purkarthofer et al., 2007). In addition, these enzymes can operate under high substrate concentrations, which has a beneficial effect on the economics of the process and makes it more efficient from a 'green chemistry' perspective. The first reports of HNLs date back to the 19th century (Wöhler and Liebig, 1837) and early 20th century (Rosenthaler, 1908). After a century several HNLs, as *Pa*HNL and *Hb*HNL, were firmly established in the industry

* Corresponding author.
E-mail address: Katarzyna.Szymanska@polsl.pl (K. Szymańska).

https://doi.org/10.1016/j.cherd.2026.06.050
Received 20 April 2026; Received in revised form 17 June 2026; Accepted 25 June 2026
Available online 25 June 2026
0263-8762/© 2026 The Authors. Published by Elsevier Ltd on behalf of Institution of Chemical Engineers. This is an open access article under the CC BY license (http://creativecommons.org/licenses/by/4.0/).

(Hanefeld, 2013). However, other HNLs derived from different organisms are still the subject of academic research. Recently, an *(R)*-selective HNL from *Granulicella tundricola* (*Gt*HNL), an aerobic bacterium found in the soil of Arctic alpine tundra was discovered (Rawat et al., 2014; Hajnal et al., 2013). It has been modified by mutagenesis at three amino acids, *Gt*HNL-A40H/V42T/Q110H (*Gt*HNL-3V) (Fig. 1), resulting in higher activity and more tightly bound cofactor compared to the wild type (Wiedner et al., 2015). The *Gt*HNL-3V, consisting of 131 amino acids, with a predominance of nonpolar side chains, including aliphatic and aromatic amino acids (74 amino acids), contributing to the stability of enzyme structure (**pdb database, 4UXA**).

From an engineering perspective, the ability to separate and reuse the catalyst is extremely important, which is why enzyme immobilisation is so widely used. Furthermore, selecting the appropriate immobilisation methods and conditions (biocatalyst engineering) allows for improved biocatalysts efficiency and/or stability. *Gt*HNL was successfully immobilised on a commercial Celite-R633 (Coloma et al., 2020, 2022). Celite-R633 belongs to the group of silica carriers with a hydrophilic surface. Given the structure of *Gt*HNL-3V, and in particular the number of amino acids with hydrophobic properties, deposition on a carrier with a hydrophilic surface may adversely affect the enzyme-carrier (guest-host) interactions and thus the conformation and ultimately the activity and stability of the enzyme (Tong et al., 2025).

These confirmational effects on the enzyme structure were previously observed for lipases which, like *Gt*HNL-3V, displays many nonpolar/hydrophobic amino acids (Kowalczykiewicz et al., 2021; Li et al., 2013). The activity of lipases immobilised on silica functionalised with hydrophilic groups was significantly lower than that of the lipases immobilised on silica modified with hydrophobic groups (Garmroodi et al., 2016; Vescovi et al., 2016). However, it was also shown that the introduction of only hydrophobic groups promoted the leaching of the enzyme from the support during the process, especially when the process was carried out in an aqueous medium. This was also observed for *Gt*HNL (Coloma et al., 2022). The leaching of lipases was counteracted using bifunctionalised silica (Kowalczykiewicz et al., 2021). Bifunctionalised silica containing both hydrophobic groups (e.g. *n*-octyl), which are responsible for the correct conformation of the enzyme, and reactive groups (e.g.: amino, epoxy), which allow the formation of a covalent bond between host and guest, thus preventing the leaching of the enzyme (Kowalczykiewicz et al., 2021; Vescovi et al., 2016; Hirata et al., 2016).

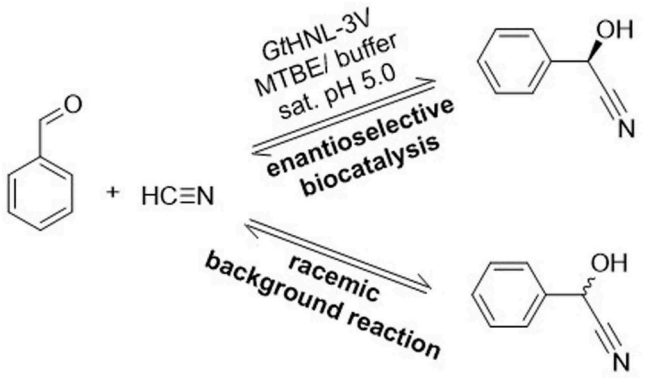
In addition, earlier research has demonstrated that the chemical character of the carrier surface has a strong influence on the local concentrations and the partitioning of the substrate and product. This can then again influence diffusion of the substrate and parameters, such as activity and K_M (Cantone et al., 2013; Kallenberg et al., 2005; Rotticci et al., 2000). Apolar or bipolar carriers might therefore positively influence biocatalytic reactions by favourable effects on the structure and stability of the enzyme and improved kinetics due to partitioning effects.

Furthermore, it has been proven that, in the synthesis of mandelonitrile from benzaldehyde (Scheme 1), silica carriers catalyses an undesirable background reaction that significantly reduces the purity of the obtained product (Stradomska et al., 2022; Van Der Helm et al., 2019).

Considering the structure and surface polarity of the enzyme (Fig. 1) and the activity of silica in the reaction, it is appropriate to modify this carrier to firstly increase the enzyme's stability and kinetics, and secondly minimise the background reaction.

Two types of silica carrier were used: mesostructured cellular foams (MCFs) (Fig. 2**a**) and silica monoliths (MHs) (Fig. 2**b**) both functionalised with *n*-octyl (O), amine (A) and epoxy (E) groups in the following configurations MCF-A, MCF-E, MCF-O, MCF-AO, MCF-EO and MH-A, MH-O, MH-AO. MCF matrices are fine powders and their process application is mainly limited to batch reactors (Szymańska et al., 2007).

Achieving high substrate conversion levels in batch reactors requires relatively long residence times. However, when it comes to chiral cyanohydrins synthesis using *Gt*HNL-3V immobilised on a silica support, this can result in low selectivity due to unfavourable background reactions. Therefore, the second step was transferring the optimal immobilisation conditions to monolithic silica (MH) supports that can be used as cores for microreactors operating in a continuous system. The possibilities and advantages of using monolithic microreactors in bio/chemical synthesis have been reviewed recently (Lambarska et al., 2024). Monolithic silica microreactors have also been successfully used in the synthesis of chiral cyanohydrins (Stradomska et al., 2022; Van Der Helm et al., 2019). However, the aforementioned work used



Scheme 1. Enantioselective synthesis of *(R)*-mandelonitrile catalysed by immobilised *Gt*HNL-3V and racemic background reaction catalysed spontaneously by silica carriers themselves.

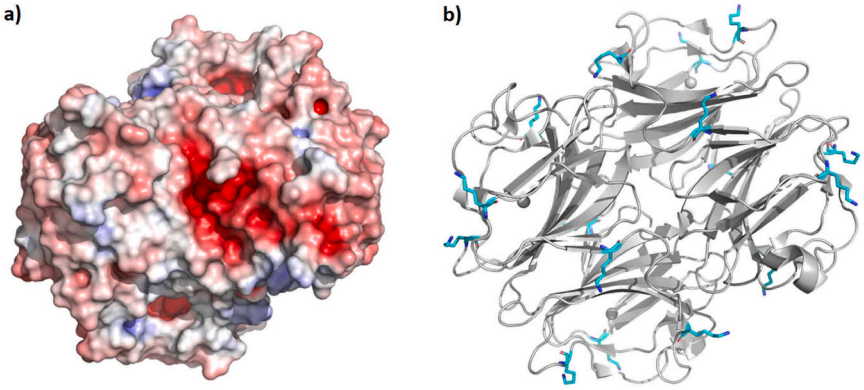


Fig. 1. *Gt*HNL-3V tetramer structure, 7.1 nm (71 Å). a) Surface polarity; red regions: negative, blue: positive charges, b) Surface lysine residues are highlighted in cyan. Structural data 4UXA was obtained from PDB database and the images were created using the PyMOL Molecular Graphics System.

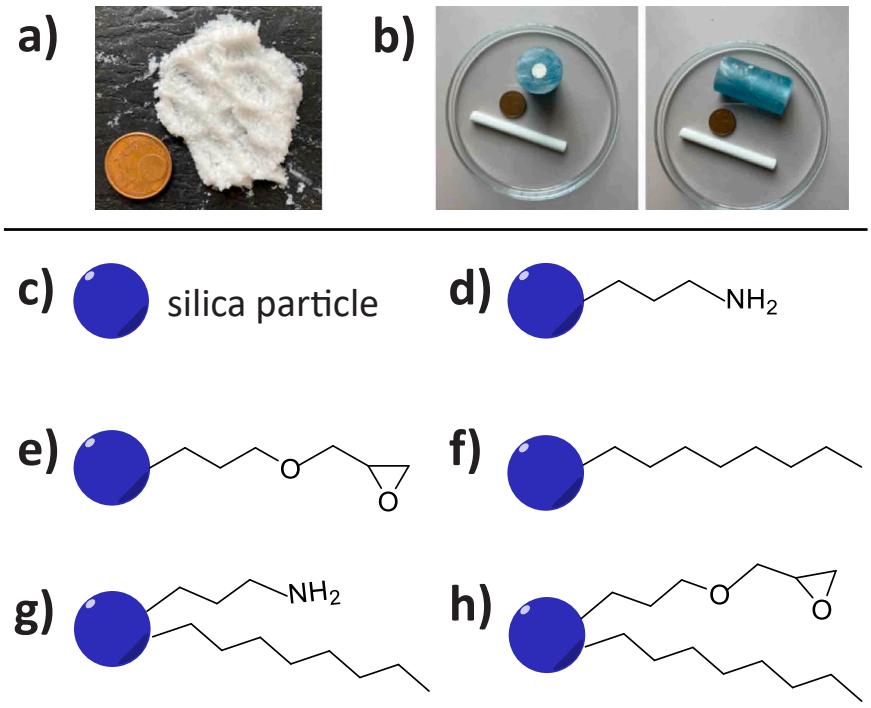


Fig. 2. a) photo of MCF silica carrier, b) silica monolith (MH) and monolithic structured microreactor, c) scheme of pure silica particle, and silica modified with d) amine (A) groups, e) epoxy (E) groups, f) *n*-octyl (O) groups, g) bifunctionalised with amine and *n*-octyl (AO) groups, h) and epoxy and *n*-octyl (EO) groups.

lyases from other organisms with entirely different structures and the silica monoliths were functionalised with amino groups, which only allow for covalent binding of hydroxynitrile lyases (Stradomska et al., 2022; Van Der Helm et al., 2019). In analysing the continuous process, the impact of shear stresses generated during the flow of reagents on the activity and stability of immobilised enzymes will be examined (Pisapia et al., 2022; Bekard et al., 2011).

2. Results and discussion

2.1. Characterisation of silica supports

Mesostructured cellular foams (MCF) (Fig. 2**a**) are formed by templating with an oil-in-water microemulsion combined with a sol-gel process (Szymańska et al., 2007), whereas silica monoliths (MH) were prepared by phase separation combined with a sol-gel process (Szymańska et al., 2016). In both cases, tetraethoxysilane was used as the silica precursor, so that the resulting materials have the same surface chemistry and differ only in the structure. Therefore, immobilisation parameters for MCF can directly be translated to the monoliths (Stradomska et al., 2022; Van Der Helm et al., 2019; Kowalczykiewicz et al., 2022). The MCF support is a fine-grained material (grain size does not exceed 100 μm) characterised by an S_{BET} specific surface area of 600 $m^2\ g^{-1}$ (Table 1) and pores in the range of 20–30 nm, significantly larger than the 7.1 nm of the enzyme. The specific surface area of silica monoliths (MH) is approximately 300 $m^2\ g^{-1}$ and the material is characterised by mesopores of approximately 20 nm and flow-forming macropores of 20–50 μm. The silica carriers were functionalised using the following organosilanes: (3-aminopropyl)trimethoxysilane (precursor of amino (A) groups), (3-glycidyl)trimethoxysilane (precursor of epoxy (E) groups) and *n*-octyltriethoxysilane (precursor of *n*-octyl (O) groups).

Table 1
Properties of MCF carriers bi-/functionalised by specific functional groups.

Carrier	S_{BET} [m^2g^{-1}]	Pore size [nm]	C/H/N [mass %]	Water retention [%]
MCF	580	27	-	4.32
MCF-A	450	23	3.66/1.33/1.08	2.46
MCF-AO	440	20	7.41/1.84/0.37	1.05
MCF-E	350	22	3.91/1.04/0	1.47
MCF-EO	450	20	2.23/0.86/0	1.87
MCF-O	440	19	5.12/1.42/0	1.67

The introduction of functional groups on the surface of the silica supports resulted in a decrease in the value of the specific surface area, while the size of the mesopores remained essentially unchanged (Table 1). The post-synthesis modification of the silica did not negatively affect the structure of the supports, as evidenced by the shape of the adsorption isotherm after functionalisation (Fig. S1).

The presence of functional groups on the silica surface was also confirmed by FT-IR spectroscopy (Fig. S2) and elemental analysis (Table 1). The content of the three basic elements (C, H, N), which are the building blocks of the functional groups, was determined. The MCF-AO and MCF-O samples have the highest carbon content, mainly due to the introduction of *n*-octyl groups. The relatively low carbon content in the MCF-EO sample indicates a low degree of functionalisation of this support (Table 1).

The amount of water adsorbed on the prepared supports was also determined (Table 1). This value can indirectly indicate the hydrophobic nature of the surface of the modified supports. In general, a higher value of adsorbed water indicates the hydrophilic nature of the support, while a decrease in the amount of adsorbed water indicates an increase in the hydrophobicity of the support surface. It was found that the introduction of functional groups, even those not considered to have hydrophobic properties (amine: MCF-A, epoxy: MCF-E), resulted in a significant reduction in the amount of water adsorbed. The analyses carried out show that the support with the lowest water content is silica functionalised with both amine and *n*-octyl groups (MCF-AO). MCF-E, MCF-EO and MCF-O supports are characterised by similar amounts of adsorbed water.

2.2. Synthesis of (R)-mandelonitrile in batch system

Appropriate biocatalysts were prepared using functionalised MCF silica carriers. Two immobilisation methods were employed: enzyme adsorption onto the MCF-O carrier, and covalent bonding onto the following carriers: MCF-A, MCF-E, MCF-AO and MCF-EO. Supports containing an amino group on their surface required activation with glutaraldehyde. During immobilisation, the mass ratio of protein to support was kept at 1:16 mg mg^{-1} and the enzyme's specific activity and concentration were maintained at 16 mg^{-1} and 10 $mg\ mL^{-1}$, respectively. It was observed that the lowest amount of protein (within the range of 30 $mg_{protein}g^{-1}_{silica}$) was bound to carriers with an epoxy group (MCF-E and MCF-EO; see Table 2**, row 1**). This may be attributed to (i) the low degree of functionalisation of the MCF-E and MCF-EO supports (cf. Table 1) and/or (ii) the propensity of glutaraldehyde, used to activate surface amino groups (MCF-A, MCF-AO), to polymerise and form branched structures, thereby increasing the number of available anchoring sites and enabling higher enzyme loading (Kim et al., 2004). A detailed discussion of immobilisation via amino and epoxy functionalities is provided in the Supporting Information.The other carriers (MCF-A, MCF-AO and MCF-O) bound approximately 40–45 $mg_{protein}g^{-1}_{silica}$. The prepared biocatalysts were tested in the synthesis of (*R*)-mandelonitrile from benzaldehyde (see Scheme 1) in a batch reactor. A similar amount of heterogeneous biocatalyst (41–52 mg) was used in the reaction. Catalysts based on MCF-E and MCF-EO carriers displayed the lowest activity (Table 3, row 1–3), in terms of both the amount of product in relation to the amount of heterogeneous catalyst (Table 3, row 1) and in relation to the amount of immobilised protein (Table 3, row 2). These catalysts also exhibited the poorest selectivity (Table 3, row 3), with an enantiomeric excess of 60–80%. Such a low enantioselectivity indicates a significant contribution of the background reaction, which is catalysed by the carrier itself. Preliminary studies indicated that the MCF-E and MCF-EO carriers exhibited significant activity in the undesirable background reaction, comparable to that of unmodified silica (MCF) (Fig. S3). Significantly better results were obtained with biocatalysts based on carriers modified with amino and *n*-octyl groups (MCF-A, MCF-O and MCF-AO; see Table 3, row 1–3). They all showed a similar degree of product yield, with the purity of the product ranging from 90% to 95%. Therefore, it can be concluded that surface modification through the introduction of amino and n-octyl groups stabilises the enzyme, resulting in enhanced catalytic activity compared with biocatalysts based on epoxy-functionalised silica supports. In enzyme-catalysed processes, two stages of catalysis influence the speed of the process: the chemical/catalytical step and the product release step (Szymańska et al., 2021). The results obtained suggest that introducing two types of functional group (amino and *n*- octyl) onto the silica surface accelerates one or both of these steps simultaneously. However, it is more likely that the product release step is accelerated, since accelerating the catalysis step typically involves altering the structure of the active site (Szymańska et al., 2021). Furthermore, as previously mentioned, the chemical nature of the carrier surface strongly influences the local concentrations and partitioning of the substrate and product (Cantone et al., 2013).

Enantiomeric purity is of great importance to the pharmaceutical and fine chemical industries as it enables the production of single-enantiomer products, thereby reducing waste generation and eliminating the need for downstream enantiomer separation. In this context, improving enantiomeric excess is not only a matter of reaction chemistry but also a key biocatalyst engineering objective, as ee can be strongly affected by the immobilisation strategy, enzyme surface density, and the local microenvironment created at the carrier interface (Hanefeld, 2013; Bolivar et al., 2022). Two approaches were therefore considered. Lowering the reaction temperature, as suggested by Wiedner et al. (2015), or increasing the amount of protein (Costes et al., 1999) on the carrier surface to minimise contact between the reagents and the carrier surface, thereby eliminating the undesirable background reaction.

Lowering the temperature significantly improved the enantiomeric excess (see Table 3, row 4–6). An enantiomeric excess of over 95% was obtained for biocatalysts based on MCF-A and MCF-AO carriers. Once again, the lowest enantiomeric excess was obtained for catalysts based on MCF-E carriers, though an improvement was also observed in this case. As expected, lowering the temperature resulted in a slightly slower product formation. For example, for the MCF-AO catalyst, the process rate expressed per amount of biocatalyst was 0.114 $mM/mg_{biocat.}{\cdot}min^{-1}$ at 23 C and decreased to 0.063 $mM/mg_{biocat.}{\cdot}min^{-1}$ at 10°C (Table 3, rows 1 and 4).

Another way to increase the enantiomeric excess was to introduce a larger amount of protein onto the carrier. Therefore, during immobilisation, a protein-to-carrier mass ratio of 1:10 mg mg^{-1} was employed. This approach increased the amount of protein bound to the carriers (see Table 2**, row 2**), and increased activity units while the trends observed during immobilisation at a lower enzyme concentration (**see** Table 2**, row 1**) remained. As before, the MCF-E and MCF-EO carriers bound the least amount of enzyme (Table 2**, row 2**), and these heterogeneous biocatalysts also exhibited the lowest enantiomeric excess (approx. 90%) and activity (Table 3, row 7–9). For biocatalysts based on other carriers (MCF-A, MCF-AO and MCF-O), the enantiomeric excess was above 96%; even for the MCF-A-based catalyst, it was close to 99% (Table 3, row 9).

Increasing the enzyme loading on the support also resulted in a slight increase in the production of (*R*)-mandelonitrile. Specifically, the rate of (*R*)-mandelonitrile formation per gram of heterogeneous biocatalyst (i.e., the mass of the support with immobilised enzyme) was approximately 0.122 and 0.133 mM $mg^{-1}{}_{biocat.}min^{-1}$ for MCF-AO and MCF-O, respectively (Table 3, row 7), whereas at the lower enzyme loading the corresponding values were 0.114 and 0.116 mM $mg^{-1}{}_{biocat.}min^{-1}$ (Table 3, row 1). At the same time, a decrease in the reaction rate expressed per mg of immobilised enzyme was observed (Table 3, row 8), which may indicate that a fraction of the enzyme deposited on the support did not participate in the catalytic process. Overall, a higher protein loading on the support primarily enabled more effective suppression of the background reaction and increased the product formation rate.

To probe the stability of the biocatalyst, the activity of all heterogeneous biocatalysts was determined after four and eight weeks of storage in buffer at pH 7 and 4°C (see Fig. S9). While all catalysts showed activity after 8 weeks, it was slightly lower than the initial activity. Importantly, the enantioselectivity of the process remained stable over the entire storage period, with enantioselectivity values consistently comparable to those observed at the initial time point.

Table 2
Protein (*Gt*HNL-3V) loading per g of silica carrier (MCF), immobilisation yield and number of enzyme units in the (*R*)-mandelonitrile synthesis in the batch process.

	mass ratio protein/ support [mg mg^{-1}]		Heterogeneous biocatalyst				
			MCF-A	MCF-AO	MCF-E	MCF-EO	MCF-O
1.	1:16	Protein load [$mg_{protein}g^{-1}_{silica}$]	39.07	43.06	28.76	31.26	45.75
		Immobilisation yield [%]	65	71	43	53	75
2.	1:10	Protein load [$mg_{protein}g^{-1}_{silica}$]	70.47	76.61	47.14	56.28	73.77
		Immobilisation yield [%]	69	75	46	55	72

Table 3
Reaction rates for the synthesis of (R)-mandelonitrile in a batch system, expressed per mg of biocatalyst or per mg of protein, as a function of protein loading and temperature. Detailed data are provided in the Supporting Information.

	mass ratio prot./car. [mg mg^{-1}]	Reaction rate/ enantiomeric excess	Heterogeneous biocatalyst				
			MCF-A	MCF-AO	MCF-E	MCF-EO	MCF-O
1.	**1:16**	[mM $mg^{-1}_{biocat.}$ min^{-1}]	0.087	0.114	0.055	0.068	0.116
2.	**23°C**	[mM $mg^{-1}_{prot.}$ min^{-1}]	2.22	2.64	1.92	2.18	2.54
3.		ee_R [%]	94–95	91–92	63–74	70–81	83–89
4.	**1:16**	[mM $mg^{-1}_{biocat.}$ min^{-1}]	0.054	0.063	0.024	0.043	0.0842
5.	**10°C**	[mM $mg^{-1}_{prot.}$ min^{-1}]	1.11	1.22	0.74	1.11	1.86
6.		ee_R [%]	98	96	82–83	92–93	92–93
7.	**1:10**	[mM $mg^{-1}_{biocat.}$ min^{-1}]	0.089	0.122	0.057	0.058	0.133
8.	**23°C**	[mM $mg^{-1}_{prot.}$ min^{-1}]	1.26	1.60	1.21	1.03	1.80
9.		ee_R [%]	99	98	90–91	90–91	96–97

2.3. Synthesis of (R)-mandelonitrile in flow system

The form of the biocatalyst usually dictates the type of reactor configuration employed. For biocatalysts based on fine-grained MCF-type particles, stirred tank reactors are most commonly used. The application of batch reactors is associated with a low catalyst-to- volume ratio, resulting in the long residence times necessary to achieve high substrate conversion (Lambarska et al., 2024; Szymańska et al., 2021). For (*R*)-mandelonitrile synthesis using *Gt*HNL-3V immobilised on silica powders, a long contact time between the carrier and the reagents can result in low product purity due to background reactions, as observed earlier (Stradomska et al., 2022; Van Der Helm et al., 2019). Flow microreactors allow for favourable catalyst-to-volume ratios, minimising contact time between reagents and substrate. From a green and safety perspective, flow reactors process only a small volume of reaction mixture at any given time, thereby minimising the quantity of chemicals, improving process safety (Vieira et al., 2025). Importantly, microreactors, especially those with tortuous channels, intensify heat and mass transfer processes significantly affecting the reaction rate (Lambarska et al., 2024; Szymańska et al., 2021). The transition from powder-based batch systems to monolithic microreactors represents a significant step in process intensification, as the hierarchical pore structure effectively decouples the trade-off between high surface area and hydraulic resistance.

While it is possible to create a packed-bed microreactor using MCF-based catalysts as the filler material, the very small particle size (with a Sauter mean diameter in the range of 5–9 μm) results in high pressure drop and bed compression. Stable silica monoliths (MH) with a hierarchical pore structure, which have a tortuous pore size of 20–50 μm were applied, as they avoid the high pressure drop and bed compression. The surface chemistry of MCF and MH is similar, so the same immobilisation parameters were used (Stradomska et al., 2022; Van Der Helm et al., 2019; Kowalczykiewicz et al., 2022). The monoliths were therefore modified with an amino group (MH-A), and *n*-octyl group (MH-O), or both an amino and *n*-octyl group (MH-AO). Cylindrical monoliths with a diameter of 6 mm and a length of 40 mm were used. Analyses showed that 9.7 mg (MH-A), 10.9 mg (MH-O) and 16.2 mg (MH-AO) of protein bound to the carriers, equivalent to 256 U, 287 U and 427 U, respectively. Microreactors based on these monoliths were tested under variable flow conditions (i.e. variable process time) to determine the efficiency and selectivity of the obtained product. The process was carried out at flow rates ranging from 0.02 mL min^{-1} to 0.46 mL min^{-1}, generating residence times of approximately 40–2 min. In all reactor types, the substrate conversion decreased with increasing flow rate, which is related to the residence time of the reagents in the microreactor (Fig. 3). The smallest changes were observed in the MH-O microreactor, for which the substrate conversion at a residence time of 2 min was approximately 70% (Fig. 3**c**). For the other microreactors (MH-A and MH-AO), the substrate conversion was 40–50% at the same residence time. Remarkable space-time yields (STY) were obtained for all types of microreactor: 38–367, 39–245 and 30–503 g L^{-1} h^{-1} in MH-A, MH-AO and MH-O, respectively. Very high purity of the resulting product was also observed in all types of reactors. However, a slight decrease in product purity was observed with an increase in the flow rate for the MH-A and MH-AO microreactors (Fig. 3). This effect was also observed in our previous work and may be related to the shear forces generated when reagents flow through the microreactor structure (Stradomska et al., 2022). Generally, higher flow rates generate greater shear forces (Pisapia et al., 2022), which can affect the conformation of the enzyme and consequently affect the accessibility of its active site for the

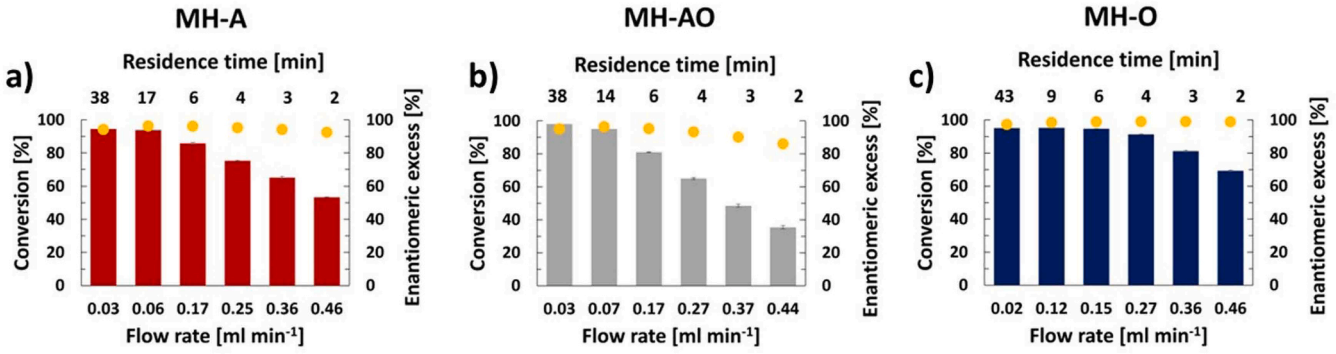


Fig. 3. Synthesis of (R)-mandelonitrile in flow process via GtHNL-3V immobilised inside silica monoliths: a) MH-A, flow velocity 0.11–1.63 cm min^{-1}, b) MH-AO, flow velocity 0.11–1.56 cm min^{-1}, c) MH-O, flow velocity 0.07–1.63 cm min^{-1}. Conversion (bars)/ enantiomeric excess (spots) vs. flow rate/residence time (min). Reaction conditions: 0.25 M benzaldehyde in MTBE, 0.75–1 M HCN in MTBE saturated with citrate phosphate buffer (50 mM, pH 5.0), 0.075 M mesitylene as internal standard, 0.075 M 1,3,5-triisopropylbenzene as second internal standard, room temperature (23°C). The amount of immobilised enzyme was: a) 9.72 mg, 256 U; b) 16.22 mg, 427 U, c) 10.91 mg, 287 U. Error bars represent the standard deviation of three independent samples (n = 3).

substrate (Bekard et al., 2011). In turn, impeded access to the active site can have an adverse effect on the selectivity of the process. However, this effect was not observed for the MH-O microreactor: even at the highest flow rates, an extremely pure product was obtained (Fig. 3). Probably the high enantioselectivity in this system is directly related to the nature of the support surface and the reaction environment. This also suggests that the octyl groups on the silica carrier's surface can stabilise the enzyme structure so effectively that it remains insensitive to increased shear forces. Due to the specific nature of the flow reactor high shear forces can occur. The hydrophobic surface functional groups stabilise the enzyme attached to the surface, protecting it from the negative effects of these forces. In the batch processes described in Section 2.2, the heterogeneous biocatalyst granules move with the fluid; therefore, the stresses at the liquid-solid interface are negligible.

The use of a hydrophobic support surface (*n*-octyl groups) in a nonpolar solvent within a monophasic system enhances the effective enantioselectivity (Rotticci et al., 2000). Initially, this type of reactor (MH-O) exhibited high process stability (Fig. 4**c**). However, if the system is stopped intermittently (overnight) and stored in buffer solutions before being reapplied, some loss of activity is observed, which then decreased rapidly. After 13 h of operation, its activity was only 20% of the initial level. This is due to the adsorption method of enzyme immobilisation, which is characterised by weak enzyme–carrier interactions (Cantone et al., 2013; Hartmann and Kostrov, 2013). The MH-A and MH-AO microreactors demonstrate significantly better process stability (see Figs. 4**a and** 4**b**), even though more process pauses with storage in buffer were performed. The former retained 40% of its initial activity after 34 h of operation (Fig. 4**a**). A decrease in both activity and enantioselectivity of the enzyme was observed. The MH-AO microreactor exhibited much better stability, still showing 50% of its initial activity after 42 h of operation (Fig. 4**b**). However, a slight decrease in selectivity was also observed in this case. It has been established that the shear stability of a protein molecule depends on the magnitude of shear forces and the duration of its application, as well as the viscosity of its surrounding medium (Bekard et al., 2011). Prolonged shear stress, as they occur in monoliths, can negatively affect the enzyme's structure, and consequently its activity and selectivity. The simultaneous introduction of amino and *n*-octyl groups was found to significantly extend the lifetime of the microreactor, indicating better stabilisation of the enzyme structure.

While all systems work well initially in buffered organic solvents, long term stability with intermittent storage showed that MH-AO outperformed the other carriers. Covalent binding suppressed any loss of enzyme and thus activity. Additionally, the *n*-octyl-groups protect the enzyme against shear forces ensuring long catalyst lifetimes.

A comparison between batch and continuous-flow configurations can, in principle, be made on the basis of the space–time yield (STY). In the present study, the two reactors were operated under the following regimes. Batch reactor (MCF-AO): substrate concentration 0.5 M, reactor volume 2 mL, enzyme amount 3.8 mg, and process time 1 h. Continuous-flow reactor (MH-AO): substrate concentration 0.25 M, reactor (void) volume 0.9 mL, flow rate 0.1 mL min^{-1} (residence time 9 min), and enzyme amount 7 mg. Under these conditions, STY values of 50 g L^{-1} h^{-1} and 151 g L^{-1} h^{-1} were obtained for the batch and flow reactor, respectively.

The marked advantage of the continuous-flow system primarily arises from the very high biocatalyst-to-reactor-volume ratio, which is difficult to achieve in a batch setup due to mixing limitations. Notably, the flow reactor was operated at a twofold lower substrate concentration than the batch system, which compromises the direct comparability of the STY values. It is highly probable that performing the flow process at higher substrate loadings could further enhance the overall productivity. This improvement of flow over batch is in line with earlier reports (Lambarska et al., 2024). The E-factor of approx. 22 g_{waste} $g_{product}^{-1}$, is low for laboratory-scale continuous flow synthesis in organic solvents (Lambarska et al., 2024). Overall, the continuous-flow setup provides clear advantages in terms of process safety and intensification.

3. Conclusions

*Gt*HNL-3V was successfully immobilised on modified silica carriers and used as a catalyst for the batch and flow syntheses of (*R*)-mandelonitrile. Supports with different surface modifications were employed; those modified with amino (A) or *n*-octyl (O) groups, or both simultaneously (bifunctionalised, AO), exhibited the greatest efficiency in both processes. Bifunctionalised carriers deserve special attention, as this modification enables the enzyme to be covalently bound (via amino groups activated with glutaraldehyde) and stabilises its structure through *n*-octyl groups. From a biocatalyst engineering perspective, this dual-functional interface creates a unique microenvironment that balances rigid multipoint covalent anchoring with hydrophobic shielding, effectively preventing enzyme leaching and deactivation. Additionally, the beneficial effect of the *n*-octyl groups was observed to manifest slightly differently in batch and flow reactors. In a batch reactor, they allowed an increase in the reaction rate, most likely by accelerating the product release stage or the partitioning of the substrate and product. In a flow reactor, the presence of hydrophobic groups improved the stability of the enzyme during the process and protected it from the adverse effects of shear forces. This shift in performance underlines the importance of bioreactor engineering, where the catalyst's mechanical robustness must be harmonised with the hydrodynamic profile of the system to maintain long-term operational stability. Furthermore, using a flow microreactor significantly reduced the time required for complete substrate conversion and decreased the reaction volume. Complete conversion was achieved in 1 h in the batch system, whereas in the continuous process, it was achieved in a few minutes. The transition from diffusion-limited batch conditions to a flow regime characterised by enhanced mass transfer rates allowed for a substantial increase in space-time yield. Reducing the volume of the flow microreactor not only allows for a favourable surface-to-volume ratio but also increases safety by minimising the potential release of hydrogen cyanide and solvent consumption.

Overall, these findings confirm that bifunctional carriers are a versatile approach to enhance the performance of hydroxynitrile lyases and potentially other enzymes in sustainable synthetic processes. By combining amine and hydrophobic groups, bifunctional carriers enable stable covalent binding, intensified catalysis, and greener reaction conditions. This work provides a robust platform for the efficient, safe, and selective synthesis of chiral cyanohydrins, with broader applicability in other enzymatic transformations, including biphasic systems.

4. Materials and methods

4.1. General

All chemicals were obtained in the highest available purity from Merck unless reported otherwise. *n*-octyltriethoxysilane from abcr GmbH was used as one of the precursors of functional groups. Toluene (97%) from VWR was used as an organic solvent. Molecular sieves beads 2 mm, pore size 0.4 nm (activated before use at 300°C for 3 h), were used as a drying agent. Benzaldehyde was distilled prior to use. Potassium cyanide (KCN, 97%) was used as a cyanide source in the HCN solution.

Caution: Hydrogen cyanide (HCN) and potassium cyanide (KCN) are highly poisonous chemicals. All experiments involving these two substances were performed in a ventilated fume hood with two calibrated HCN detectors (inside and outside the fume hood). The HCN wastes were neutralised over a large excess of commercial bleach (15% sodium hypochlorite solution) for disposal.

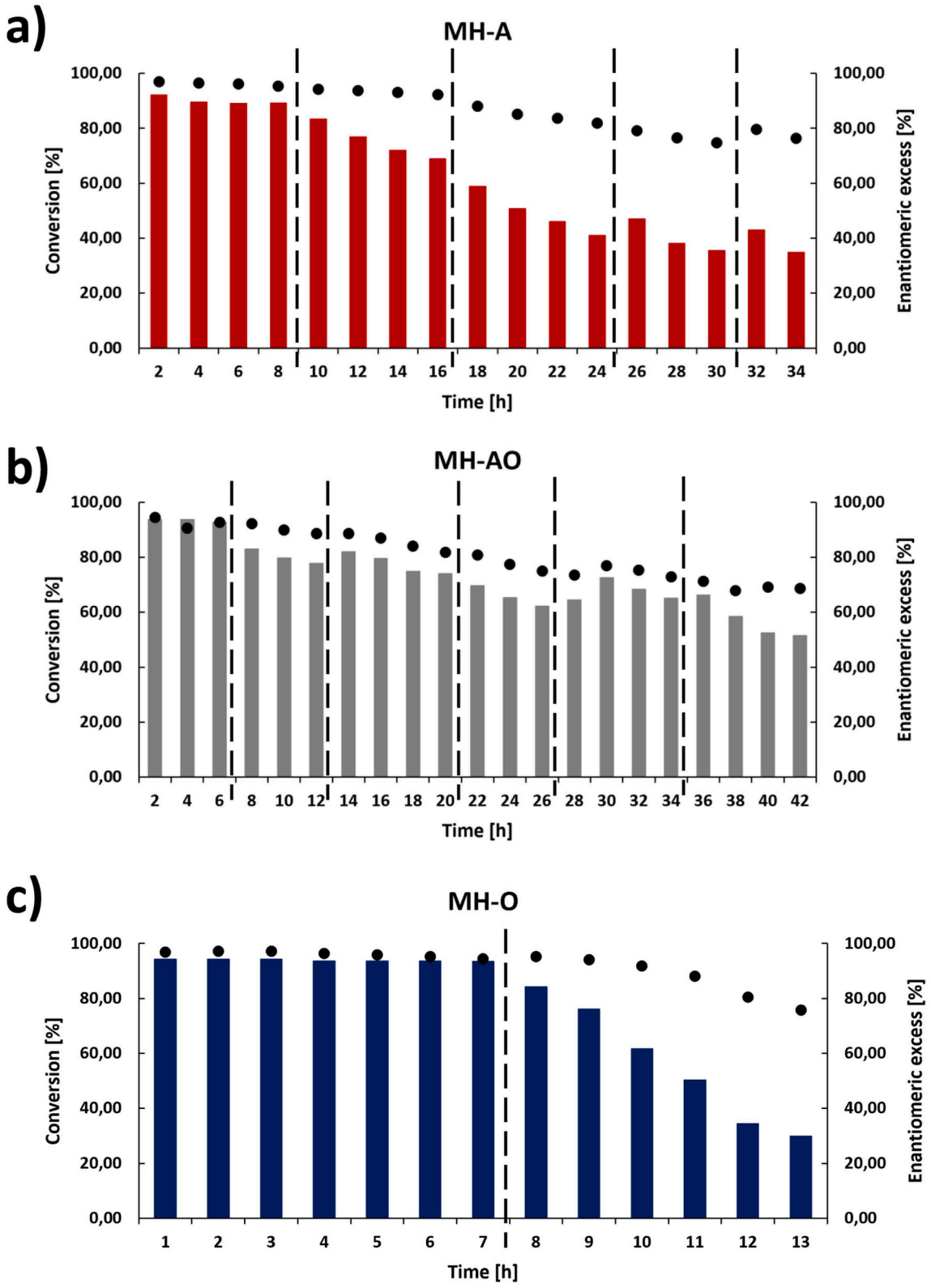


Fig. 4. Stability of *Gt*HNL-3V immobilised on a) MH-A, b) MH-AO and c) MH-O in (*R*)-mandelonitrile synthesis in flow conditions. Conversion (bars)/enantiomeric excess (spots) vs. time (h). Reaction conditions: 0.25 M benzaldehyde in MTBE, 0.75–1 M HCN in MTBE saturated with citrate phosphate buffer (50 mM, pH 5.0), 0.075 M mesitylene as internal standard, 0.075 M 1,3,5-triisopropylobenzene as second internal standard, room temperature (23°C), flow rate 0.1 mL min^{-1}. The amount of immobilised enzyme was: a) 9.72 mg, 256 U; b) 16.22 mg, 427 U, c) 10.91 mg, 287 U. The dashed lines indicate the times when the reaction was stopped, the monolith was washed with storage buffer and further reaction was initiated after overnight incubation in storage buffer.

4.2. Expression and purification of triple variant GtHNL-A40H/V42T/Q110H (GtHNL-3V)

The enzyme expression and purification was performed following the procedure describe in literature (Coloma et al., 2020) with slight modifications. The pET−28a-*Gt*HNL-3V plasmid was transformed into *E. coli* BL21(DE3) competent cells. 2 μL (100 ng) of plasmid was added into 100 μL competent cells and incubated on ice for 30 min. Transformation was indicated by heat shock at 42°C for 30 s and cooled on ice for 2 min. Then 500 μL LB-medium was added to the transformed cells and incubated (New Brunswick Scientific Incubator Shaker Excella E24 Series) for 1 h at 37°C, 180 rpm. 100 μL of incubated mixture was spread onto LB-agar plate containing kanamycin (50 μg mL^{-1}) and incubated overnight at 37°C. A preculture was prepared by inoculating one single colony of *E.coli* BL21(DE3)-pET−28a-*Gt*HNL-3V in 15 mL LB medium with kanamycin (50 μg mL^{-1}) and incubated overnight at 37°C, 180 rpm. Then this preculture was used for inoculation of 1 L Terrific Broth (TB) medium with potassium phosphate buffer (90 mM, pH 7.0) containing kanamycin (50 μg mL^{-1}) and incubated at 37°C, 180 rpm. When the OD_{600} reached 0.5–0.7 the gene expression was induced by addition 200 μL isopropylo-β-D-thiogalactioside (IPTG) (0.5 M) with a final concentration 0.1 mM IPTG. The *Gt*HNL-3V is a metal dependent cupin so addition of $MnCl_2$ (0.1 mM Mn^{2+} final concentration) is necessary. Therefore 100 μL $MnCl_2$ (1 M) was added. Culture was incubated overnight at 25°C, 180 rpm. Cells were harvested at 4°C, 5000 rpm, 20 min (Sorvall RC6, Thermo Scientific). The supernatant was discarded and the pellet was washed with 20 mL sodium phosphate buffer (10 mM, pH 7.0) at 4°C, 8000 rpm, 20 min. The supernatant was discarded and the pellet of *Gt*HNL-3V was resuspended in lysis buffer containing 30 mL potassium phosphate buffer (20 mM, pH 7.0), 0.5 mg DNase, 1 mM of $MgCl_2$ and 1 mM of phenylmethylsulfonyl fluoride (PMSF), mixed for 30 min and lysed in a cell disruptor (Constant Systems Ltd., the United Kingdom) at 1.6 kbar and 4°C. The cell free extract (CFE) was collected and centrifuged at 4°C, 5000 rpm, 20 min. The supernatant was heated during 30 min at 65°C and centrifuged at 4°C, 10000 rcf, 20 min. The purified enzyme was stored at −20°C.

4.3. Synthesis and functionalisation of MCF carriers

The MCF carrier synthesis was performed as described in the literature (Kumpf et al., 2020; Szymańska et al., 2009): 2 g of Pluronic 123 was dissolved in 60 mL of 2 M HCl and 15 mL of deionised water, after which 0.023 g (0.6 mmol) of NH_4F and 5.8 mL (41.68 mmol) of 1,3,5-trimethylbenzene (TMB) was added and stirred at 40°C, 700 rpm for 1 h under reflux. Next 4.7 mL (21 mmol) of tetraethyl orthosilicate (TEOS) was added dropwise and again stirred at 40°C, 700 rpm for 1 h. The obtained suspension was thermostated at first at 40°C for 20 h, then at 100°C for a further 24 h. Finally the suspension was left to cool down to room temperature and then filtered. The precipitate was washed with deionised water, dried at room temperature and calcined at 550°C for 8 h. Directly before functionalisation the silica carrier was subjected to water vapour adsorption for 5 h and then dried at 200°C for 3 h. The functionalisation of the prepared MCF carrier with amino, epoxide and *n*-octyl groups was carried out by mixing 1 g of dry MCF carrier with: 0.27 mL (0.28 g, 1.5 mmol) 3-aminopropyltrimethoxysilane (amino groups, MCF-A) or 0.34 mL (0.36 g, 1.5 mmol) 3-glycidoxypropyltrimethoxysilane (epoxide groups, MCF-E) or 0.49 mL (0.43 g, 1.5 mmol) *n*-octyltriethoxysilane (*n*-octyl groups, MCF-O) or 0.135 mL (0.14 g, 0.75 mmol) 3-aminopropyltrimethoxysilane and 0.245 mL (0.21 g, 0.75 mmol) *n*-octyltriethoxysilane (MCF-AO) or 0.17 mL (0.18 g, 0.75 mmol) 3-glycidoxypropyltrimethoxysilane and 0.245 mL (0.21 g, 0.75 mmol) *n*-octyltriethoxysilane (MCF-EO) in 25 mL of dry toluene. The reactions were carried out under reflux at 85°C, 500 rpm for 24 h. Then the reaction mixtures were filtered and washed with a dry toluene and finally dried in room temperature.

4.4. Synthesis and functionalisation of silica monoliths (MH)

The silica monoliths were prepare as described in the literature (Van Der Helm et al., 2019; Szymańska et al., 2013): 8.67 g of PEG 35 000 was dissolved in 100 mL of 1 M HNO_3. Then, 82.8 mL (373.6 mmol) of TEOS was added dropwise during mixing at 700 rpm in an ice bath. The solution thus obtained was stirred for another 30 min in an ice bath. After that time 3.8 g (10.4 mmol) of hexadeacyltrimethylammonium bromide (CTAB) was added and stirred for another 30 min at room temperature. Then, the mixture was poured into appropriate moulds, tightly closed and thus prepared sample was thermostated at 40°C for 10 days. Then the monoliths were impregnated with 1 M aqueous NH_3 solution at 90°C for 9 h, washed with deionised water and dried at room temperature for a week and then calcined at 550°C for 10 h. Functionalisation and bifunctionalisation protocol was similar to the data available in subsection 4.3 with slight modifications. MHs were immersed in a solution of functional groups dissolved in 40 mL of dry toluene, giving about 1.5 mmol concentration of selected groups per g of silica. Functionalisations were carried out under reflux at 85°C, 500 rpm for 72 h. After taking out the monoliths, they were washed with ethanol at 50°C for 5 h. The wet monoliths were dried at room temperature for a week and then clad with polymer resin (L285MGD-H285MGS type) to obtain single-rod microreactor 40 mm in length and 6 mm in diameter with a reactor volume of 0.96 mL.

4.5. GtHNL-3V activity assay and kinetic parameters determination

*Gt*HNL-3V activity assay was measured spectrophotometrically (Agilent Technologies Cary60 UV-Vis) using a method of monitoring the conversion of purified *rac*-mandelonitrile (60 mM) into benzaldehyde and HCN described in literature (Okrob et al., 2011). The cleavage of substrate was followed by measuring the increase in absorbance at wavelength of 280 nm, 25°C in 1 mL quartz glass cuvette. Measured specific activity values for *Gt*HNL-3V was 16.29 mg^{-1} of total protein. Unit is defined as μmol of benzaldehyde formed per minute in citrate/phosphate buffer (50 mM, pH 5.0) at 25°C.

4.6. Preparation of hydrogen cyanide

An HCN solution (1.5–2 M) in MTBE saturated with buffer was prepared as follows (Coloma et al., 2020): 25 mL of MTBE and 10 mL of deionised water were mixed in an Erlenmeyer flask in an ice bath. Then 6.51 g of potassium cyanide (KCN, 0.1 M) was added and stirred for 15 min. Next 10 mL of HCl solution (30% v/v) was added dropwise and stirring was continued. The obtained HCN solution was allowed to reach room temperature and the organic phase containing HCN was separated and collected. Separation was repeated twice more by adding 7 mL of MTBE each time. The final HCN solution was kept over citrate/phosphate buffer (50 mM, pH 5.0), in a 1:1 ratio and stored in a dark bottle at 4°C. The concentration of HCN solution in MTBE saturated with buffer was determined by titration. 1 mL of HCN solution was added to 5 mL of NaOH (2 M) in an Erlenmeyer flask and magnetically stirred for 2 min. A small amount of K_2CrO_4 was added (the solution took on a yellow colour). The solution was titrated using $AgNO_3$ (0.1 M). Cyanide reacts 1:1 with silver and precipitates. If there are no cyanide ions left in the mixture it change the colour from yellow to brown.

4.7. Enzyme immobilisation on MCF carriers

Before immobilisation 1 g of each carrier (MCF-A, MCF-AO, MCF-E, MCF-EO, MCF-O) was washed successively: once with 15 mL of ethanol, twice with 15 mL of deionised water and twice with 15 mL of phosphate buffer (Na_2HPO_4/KH_2PO_4, 100 mM, pH 7.0). After each step, the samples were centrifuged at 22°C and 8.677x*g* for 15 min. Carriers with amino groups (MCF-A, MCF-AO) were extra activated with 2.5% (V/V) glutaraldehyde solution in phosphate buffer (Na_2HPO_4/KH_2PO_4,

100 mM, pH 7.0) for 1 h. Next, excess of glutaraldehyde was washed out with deionised water and phosphate buffer (Na_2HPO_4/KH_2PO_4, 100 mM, pH 7.0). An enzyme solution was prepared in phosphate buffer (Na_2HPO_4/KH_2PO_4, 100 mM, pH 7.0) with a final protein concentration of 10 mg mL^{-1}. After completing the washing steps, 6 mL of this solution was added for low protein loading, providing 60 mg of protein and yielding an enzyme-to-carrier ratio of 1:16 (w/w). For high protein loading 10 mL of the same solution was applied, corresponding to 100 mg of protein and a ratio of 1:10 (w/w). The suspensions were gently mixed on the ENVIRO-Genie sample shaker and incubator for 2 h at 20°C and stored at 4°C overnight.

After overnight incubation, the carriers were centrifuged at 6°C and 8.677x*g* for 15 min. The supernatant (eluate) with unbound protein was collected as fractions for protein determination. The removal of unbound protein was performed by washing the carriers twice with phosphate buffer (Na_2HPO_4/KH_2PO_4, 100 mM, pH 7.0). Each wash was carried out by gentle mixing in ENVIRO-Genie at 4°C for 30 min and centrifuged as described above. The eluates were collected. After that, the enzyme immobilised on MCF-O was stored in phosphate buffer (Na_2HPO_4/KH_2PO_4, 100 mM, pH 7.0) at 4°C overnight. The enzyme immobilised on the carriers MCF-A, MCF -AO, MCF-E, and MCF-EO was further washed to remove non-covalently bound protein as follows: two times with phosphate buffer (Na_2HPO_4/KH_2PO_4, 100 mM, pH 7.0) with NaCl (500 mM), one time with acetate buffer (100 mM, pH 4.5) and several times with deionised water to remove the acid. At each step, the samples were mixed in ENVIRO-Genie for 20 min at 4°C and centrifuged as above. To hydrolyse the remaining epoxides (Dib and Nidetzky, 2008; Quan et al., 2008) (MCF-E, MCF-EO) or to create an imine bond (Colombo et al., 2016) (MCF-A, MCF-AO) carriers were suspended in Tris-HCl buffer (500 mM, pH 7.8) at 4°C overnight.

After another night, carriers in Tris-HCl buffer (500 mM, pH 7.8) were centrifuged as above and rinsed with 15 mL of phosphate buffer (Na_2HPO_4/KH_2PO_4, 100 mM, pH 7.0) by gently mixing in ENVIRO for 15 min to remove excess Tris-HCl buffer. Before the enzymatic reactions were performed, all carriers (MCF-A, MCF-AO, MCF-E, MCF-EO and MCF-O) with immobilised *Gt*HNL-3V were centrifuged as above and rinsed with 15 mL of citrate/phosphate buffer (50 mM, pH 5.0) by gently mixing in ENVIRO-Genie for 5 min and centrifuged as above. Then 400 mg samples for enzymatic reactions and dry matter determination were collected and the rest was prepared for storage. For the storage, enzymes immobilised on carriers were rinsed with 15 mL phosphate buffer (Na_2HPO_4/KH_2PO_4, 100 mM, pH 7.0), centrifuged as above and kept over the same buffer at 4°C.

To determine the amount of immobilised enzyme, the mass of unbound protein in the eluates was measured by the Lowry method (Lowry et al., 1951) using bovine serum albumin as a standard and subtracting it from the mass of the total applied protein.

4.8. Enzyme immobilisation on MH

Before immobilisation monoliths MH-A, MH-AO and MH-O were washed with ethanol and deionised water in flow condition for 60 min each (60 mL h^{-1}) and then with phosphate buffer (Na_2HPO_4/KH_2PO_4, 100 mM, pH 7.0) for 40 min (45 mL h^{-1}). Carriers with amino groups (MH-A, MH-AO) were additionally activated in flow conditions with 2.5% (V/V) glutaraldehyde solution in phosphate buffer (Na_2HPO_4/KH_2PO_4, 100 mM, pH 7.0) for 60 min (30 mL h^{-1}). Next, excess of glutaraldehyde was washed out with deionised water for 60 min (30 mL h^{-1}) and phosphate buffer (Na_2HPO_4/KH_2PO_4, 100 mM, pH 7.0) for another 40 min (30 mL h^{-1}). For immobilisation, an enzyme solution of *Gt*HNL-3V with an activity of 128 mL^{-1} and protein concentration of 9 mg mL^{-1} was used. When the washing steps were completed on each carrier, 5 mL of prepared enzyme solution was circulated through the microreactor for 120 min (20 mL h^{-1}) at room temperature and then stored at 4°C overnight.

After overnight incubation, the excess of protein was removed by phosphate buffer (Na_2HPO_4/KH_2PO_4, 100 mM, pH 7.0) for 40 min (3 mL h^{-1}) and additional 30 min (5 mL h^{-1}). The eluate with unbound protein was collected as fractions for protein determination. After that, the enzyme immobilised on MH-O monolith was stored in phosphate buffer (Na_2HPO_4/KH_2PO_4, 100 mM, pH 7.0) at 4°C overnight. The enzyme immobilised on the MH-A and MH -AO monoliths were further washed to remove non-covalently bound protein as follows: phosphate buffer (Na_2HPO_4/KH_2PO_4, 100 mM, pH 7.0) with NaCl (500 mM) for 60 min (30 mL h^{-1}), sodium acetate buffer (100 mM, pH 4.5) for 30 min (30 mL h^{-1}) and with deionised water for 60 min (30 mL h^{-1}). To create an imine bond (Colombo et al., 2016) (MH-A, MH-AO) monoliths were washed with Tris-HCl buffer (500 mM, pH 7.8) and then stored at 4°C overnight in this buffer.

Before starting the reaction, the monoliths washed with Tris-HCl buffer (500 mM, pH 7.8) were washed out with deionised water for 30 min (30 mL h^{-1}) to remove TRIS-HCl buffer and then with citrate/phosphate buffer (50 mM, pH 5.0) for 30 min (15 mL h^{-1}). The MH-O monolith was washed only with citrate/phosphate buffer (50 mM, pH 5.0) for 30 min (15 mL h^{-1}). The amount of enzyme on the carrier was calculated as above (4.7 subsection).

4.9. Batch synthesis of (R)-mandelonitrile

Before starting the process, reaction mixture was prepared in a 25 mL measuring flask: 1.33 g (0.5 M, 12.53 mmol) freshly distilled benzaldehyde and 0.225 g (0.075 M, 1.87 mmol) mesitylene were dissolved in MTBE solution containing 1.5–2 M HCN saturated with citrate/phosphate buffer (50 mM, pH 5.0). Meanwhile, 400 mg of wet MCF-A, MCF-AO, MCF-E, MCF-EO, MCF-O carriers with immobilised *Gt*HNL-3V were added to 4 mL of HPLC vials (two replicates per carrier type). Then 2 mL of prepared substrate solution was added, which started the reaction. The enzymatic reactions were conducted at room temperature (23°C) or 10°C with agitation at 300 rpm. For reactions at 23°C, samples were collected at 20, 40 and 60 min, whereas at 10°C, samples were taken at 30, 60 and 90 min. Samples (around 50 μL) were filtered and then analysed according to the method described below (4.11 subsection).

To determine the amount of biocatalyst immobilised on MCF carriers added to the reaction, the dry mass determination was carried out as follows: 400 mg of each wet carrier was weighed into a glass vessel and dried at 110°C to a solid mass.

4.10. Continuous flow synthesis of (R)-mandelonitrile

Two infusion pumps (Legato 100) equipped with glass syringes connected to a mixing unit (with a T-piece assembly) were deployed. The first one was used for pumping the 0.5 M freshly distilled benzaldehyde (1.33 g, 12.53 mmol) with 0.15 M mesitylene (internal standard I, 0.45 g, 3.74 mmol) in MTBE (25 mL). The second one was used for pumping the 1.5–2 M HCN solution in MTBE (saturated with citrate/phosphate buffer 50 mM, pH 5.0) with 0.15 M 1,3,5 -triisopropylbenzene (internal standard II, 0.77 g, 3.75 mmol, 25 mL). The combined flows mixed in a 1:1 (V/V) ratio were passed through the monoliths microreactors. The reaction was carried out at room temperature (23°C) with different flow rates for 5 h. The set flow rate was stabilised for an appropriate time (approx 6 volumes of microreactor) and then three samples for each flow rate were collected in defined time and every sample was weighted to check the flow rate (flow rate = (weight of sample/MTBE density)/collection time). Concentrations of substrate and product enantiomeric excess at different flow rate (i.e. residence times) were determined using HPLC technics.

4.11. HPLC analysis and sampling

10 μL of each sample was taken and added to the 990 μL of mobile phase heptane:2-propanol 95:5 in 1.5 mL Eppendorf tubes. A small

amount of anhydrous magnesium sulfate ($MgSO_4$) was added as a drying agent to remove water from the solution. The prepared samples were vortexed for a couple of seconds and centrifuged for 1 min at 5000 rpm. 700 µL of the supernatant was transferred to a 1.5 mL HPLC vial and 10 µL was injected into the HPLC (Chiralpak AD-H column, column size: 0.46 cm l.D x 25 cm), the flow rate was 1 mL min^{-1} and the UV detector was set at 216 nm. The column was set at 40°C and the sample in the autosampler was kept at room temperature.

Author contributions

AL conducted the investigation, developed the methodology, performed data analysis and visualisation, and prepared the original draft. UH and KS conceived the study, supervised the project, and revised the manuscript. LvdW provided guidance on enzyme expression and, together with MS, arranged shipment of the enzyme to Poland. MS provided guidance on enzyme purification and coordinated its shipment. KM performed thermogravimetric measurements, and WP performed nitrogen adsorption isotherm measurements.

CRediT authorship contribution statement

Katarzyna Szymańska: Writing – review & editing, Supervision, Conceptualization. **Wojciech Pudło:** Investigation. **Katarzyna Maresz:** Investigation. **Marc Strampraad:** Investigation. **Aleksandra Lambarska:** Writing – original draft, Resources, Methodology, Investigation, Conceptualization. **Laura van der Weel:** Investigation. **Ulf Hanefeld:** Writing – review & editing.

Declaration of Competing Interest

The authors declare that they have no known competing financial interests or personal relationships that could have appeared to influence the work reported in this paper.

Acknowledgements

The authors are grateful for generous financial support from the Ministry of Science and Higher Education (Poland) program under grant agreement PN/01/0267/2022 (The Pearls of Science for A.L.).

Appendix A. Supporting information

Supplementary data associated with this article can be found in the online version at doi:10.1016/j.cherd.2026.06.050.

References

Bekard, I.B., Asimakis, P., Bertolini, J., Dunstan, D.E., 2011. The effects of shear flow on protein structure and function. Biopolymers 95, 733–745. https://doi.org/10.1002/bip.21646.

Bolivar, J.M., Woodley, J.M., Fernandez-lafuente, R., 2022. Is enzyme immobilization a mature discipline ? Some critical considerations to capitalize on the benefits of immobilization. Chem. Soc. Rev. 6251–6290. https://doi.org/10.1039/d2cs00083k.

Bracco, P., Busch, H., Von Langermann, J., Hanefeld, U., 2016. Enantioselective synthesis of cyanohydrins catalysed by hydroxynitrile lyases-a review. Org. Biomol. Chem. 14, 6375–6389. https://doi.org/10.1039/c6ob00934d.

Cantone, S., Ferrario, V., Corici, L., Ebert, C., Fattor, D., Spizzo, P., Gardossi, L., 2013. Efficient immobilisation of industrial biocatalysts: criteria and constraints for the selection of organic polymeric carriers and immobilisation methods. Chem. Soc. Rev. 42, 6262–6276. https://doi.org/10.1039/c3cs35464d.

Coloma, J., Guiavarc'h, Y., Hagedoorn, P.L., Hanefeld, U., 2020. Probing batch and continuous flow reactions in organic solvents:Granulicella tundricolahydroxynitrile lyase (GtHNL). Catal. Sci. Technol. 10, 3613–3621. https://doi.org/10.1039/d0cy00604a.

Coloma, J., Teeuwisse, L., Afendi, M., Hagedoorn, P., Hanefeld, U., 2022. Batch and Flow Nitroaldol Synthesis Catalysed by Granulicella tundricola Hydroxynitrile Lyase Immobilised on Celite R-633. Catalysts 12, 161.

Colombo, G., Clerici, M., Garavaglia, M.E., Giustarini, D., Rossi, R., Milzani, A., Dalle-Donne, I., 2016. A step-by-step protocol for assaying protein carbonylation in biological samples. J. Chromatogr. B Anal. Technol. Biomed. Life Sci. 1019, 178–190. https://doi.org/10.1016/j.jchromb.2015.11.052.

Costes, D., Wehtje, E., Adlercreutz, P., 1999. Hydroxynitrile lyase-catalyzed synthesis of cyanohydrins in organic solvents Parameters influencing activity and enantiospecificity. Enzym. Microb. Technol. 25, 384–391. https://doi.org/10.1016/S0141-0229(99)00055-1.

Dadashipour, M., Asano, Y., 2011. Hydroxynitrile lyases: insights into biochemistry, discovery, and engineering. ACS Catal. 1, 1121–1149. https://doi.org/10.1021/cs200325q.

Dib, I., Nidetzky, B., 2008. The stabilizing effects of immobilization in D-amino acid oxidase from Trigonopsis variabilis. BMC Biotechnol. 8, 1–11. https://doi.org/10.1186/1472-6750-8-72.

Ganesh, K.N., Zhang, D., Miller, S.J., Rossen, K., Chirik, P.J., Kozlowski, M.C., Zimmerman, J.B., Brooks, B.W., Savage, P.E., Allen, D.T., Voutchkova-Kostal, A.M., 2021. Green chemistry: a framework for a sustainable future. ACS Omega 6, 16254–16258. https://doi.org/10.1021/acsomega.1c03011.

Garmroodi, M., Mohammadi, M., Ramazani, A., Ashjari, M., Mohammadi, J., Sabour, B., Yousefi, M., 2016. Covalent binding of hyper-activated Rhizomucor miehei lipase (RML) on hetero-functionalized siliceous supports. Int. J. Biol. Macromol. 86, 208–215. https://doi.org/10.1016/j.ijbiomac.2016.01.076.

Griengl, H., Hickel, A., V. Johnson, D., Kratky, C., Schmidt, M., Schwab, H., 1997. Enzymatic cleavage and formation of cyanohydrins: a reaction of biological and synthetic relevance. Chem. Commun. 1933–1940. https://doi.org/10.1039/a700907k.

Guan, X.E., Miao, R.P., Hua, X., Jin, X., Deng, G.Z., Cui, B.D., Han, W.Y., Wan, N.W., Chen, Y.Z., 2023. Biocatalytic Enantioselective Synthesis of Chiral β-Hydroxy Nitriles Using Cyanohydrins as Cyano Sources. ACS Catal. 13, 13597–13606. https://doi.org/10.1021/acscatal.3c03173.

Hajnal, I., Łyskowski, A., Hanefeld, U., Gruber, K., Schwab, H., Steiner, K., 2013. Biochemical and structural characterization of a novel bacterial manganese-dependent hydroxynitrile lyase. FEBS J. 280, 5815–5828. https://doi.org/10.1111/febs.12501.

Hanefeld, U., 2013. Immobilisation of hydroxynitrile lyases. Chem. Soc. Rev. 42, 6308–6321. https://doi.org/10.1039/c3cs35491a.

Hanefeld, U., Hollmann, F., Paul, C.E., 2022. Biocatalysis making waves in organic chemistry. Chem. Soc. Rev. 51, 594–627. https://doi.org/10.1039/d1cs00100k.

Hartmann, M., Kostrov, X., 2013. Immobilization of enzymes on porous silicas – benefits and challenges. Chem. Soc. Rev. 42, 6277–6289. https://doi.org/10.1039/c3cs60021a.

Hirata, D.B., Albuquerque, T.L., Rueda, N., Sánchez-Montero, J.M., Garcia-Verdugo, E., Porcar, R., Fernandez-Lafuente, R., 2016. Advantages of heterofunctional octyl supports: production of 1,2-dibutyrin by specific and selective hydrolysis of tributyrin catalyzed by immobilized lipases. ChemistrySelect 1, 3259–3270. https://doi.org/10.1002/slct.201600274.

Jangir, N., Padhi, S.K., 2019. Immobilized Baliospermum montanum hydroxynitrile lyase catalyzed synthesis of chiral cyanohydrins. Bioorg. Chem. 84, 32–40. https://doi.org/10.1016/j.bioorg.2018.11.017.

Kallenberg, A.I., Van Rantwijk, F., Sheldon, R.A., 2005. Immobilization of penicillin G acylase: the key to optimum performance. Adv. Synth. Catal. 347, 905–926. https://doi.org/10.1002/adsc.200505042.

Kim, J.K., Park, J.K., Kim, H.K., 2004. Synthesis and characterization of nanoporous silica support for enzyme immobilization. Colloids Surf. A Physicochem. Eng. Asp. 241, 113–117. https://doi.org/10.1016/j.colsurfa.2004.04.048.

D. Kowalczykiewicz, M. Przypis, L. Mestrom, A. Kumpf, D. Tischler, P.-L. Hagedoorn, U. Hanefeld, A. Jarzębski, K. Szymańska, Engineering of continuous bienzymatic cascade process using monolithic microreactors – In flow synthesis of trehalose, 427 (2022) 1–8.

Kowalczykiewicz, D., Szymańska, K., Gillner, D., Jarzębski, A.B., 2021. Rotating bed reactor packed with heterofunctional structured silica-supported lipase. Developing an effective system for the organic solvent and aqueous phase reactions. Microporous Mesoporous Mater. 312, 1–8. https://doi.org/10.1016/j.micromeso.2020.110789.

Kumpf, A., Kowalczykiewicz, D., Szymańska, K., Mehnert, M., Bento, I., Łochowicz, A., Pollender, A., Jarzębski, A., Tischler, D., 2020. Immobilization of the Highly Active UDP-Glucose Pyrophosphorylase From Thermocrispum agreste Provides a Highly Efficient Biocatalyst for the Production of UDP-Glucose. Front. Bioeng. Biotechnol. 8, 1–15. https://doi.org/10.3389/fbioe.2020.00740.

Lambarska, A., Szymańska, K., Hanefeld, U., 2024. Monoliths enabling biocatalysis in flow chemistry. Green. Chem. 26, 10718–10738. https://doi.org/10.1039/d4gc03535f.

Li, L., Feng, W., Pan, K., 2013. Immobilization of lipase on amino-cyclodextrin functionalized carbon nanotubes for enzymatic catalysis at the ionic liquid-organic solvent interface. Colloids Surf. B Biointerfaces 102, 124–129. https://doi.org/10.1016/j.colsurfb.2012.07.050.

Lowry, O.H., Rosebrough, N.J., Farr, A.L., Randall, R.J., 1951. Protein measurement with the Folin phenol reagent. J. Biol. Chem. 193, 265–275. https://doi.org/10.1016/s0021-9258(19)52451-6.

Lozano, P., García-Verdugo, E., 2023. From green to circular chemistry paved by biocatalysis. Green. Chem. 25, 7041–7057. https://doi.org/10.1039/d3gc01878d.

Newman, S.G., Jensen, K.F., 2013. The role of flow in green chemistry and engineering. Green. Chem. 15, 1456–1472. https://doi.org/10.1039/c3gc40374b.

Okrob, D., Paravidino, M., Orru, R.V.A., Wiechert, W., Hanefeld, U., Pohl, M., 2011. Hydroxynitrile lyase from Arabidopsis thaliana: Identification of reaction parameters for enantiopure cyanohydrin synthesis by pure and immobilized catalyst. Adv. Synth. Catal. 353, 2399–2408. https://doi.org/10.1002/adsc.201100199.

Padhi, S.K., 2017. Modern approaches to discovering new hydroxynitrile lyases for biocatalysis. ChemBioChem 18, 152–160. https://doi.org/10.1002/cbic.201600495.
Pisapia, F., Balachandran, W., Rasekh, M., 2022. Organ-on-a-Chip: Design and Simulation of Various Microfluidic Channel Geometries for the Influence of Fluid Dynamic Parameters. Appl. Sci. 12. https://doi.org/10.3390/app12083829.
Purkarthofer, T., Skranc, W., Schuster, C., Griengl, H., 2007. Potential and capabilities of hydroxynitrile lyases as biocatalysts in the chemical industry. Appl. Microbiol. Biotechnol. 76, 309–320. https://doi.org/10.1007/s00253-007-1025-6.
Quan, L., Wei, D., Jiang, X., Liu, Y., Li, Z., Li, N., Li, K., Liu, F., Lai, L., 2008. Resurveying the Tris buffer solution: the specific interaction between tris(hydroxymethyl) aminomethane and lysozyme. Anal. Biochem. 378, 144–150. https://doi.org/10.1016/j.ab.2008.04.006.
Rawat, S.R., Männistö, M.K., Starovoytov, V., Goodwin, L., Nolan, M., Hauser, L., Land, M., Walston Davenport, K., Woyke, T., Häggblom, M.M., 2014. Complete genome sequence of Granulicella tundricola type strain MP5ACTX9T, an Acidobacteria from tundra soil. Stand. Genom. Sci. 9, 449–461. https://doi.org/10.4056/sig.
Rosenthaler, L., 1908. Ueber die Bildung des Bittermandelöls. Biochem. Z. 14, 238–253. https://doi.org/10.1002/andp.18371170611.
Rotticci, D., Norin, T., Hult, K., 2000. Mass transport limitations reduce the effective stereospecificity in enzyme-catalyzed Kinetic Resolution. Org. Lett. 2, 1373–1376. https://doi.org/10.1021/ol005639m.
Sheldon, R.A., Brady, D., 2022. Green chemistry, biocatalysis, and the chemical industry of the future. ChemSusChem 15, e202102628.
Sheldon, R.A., Pereira, P.C., 2017. Biocatalysis engineering: the big picture. Chem. Soc. Rev. 46, 2678–2691. https://doi.org/10.1039/c6cs00854b.
Stradomska, D., Coloma, J., Hanefeld, U., Szymańska, K., 2022. Continuous flow for enantioselective cyanohydrin synthesis. Catal. Sci. Technol. 12, 3356–3362. https://doi.org/10.1039/d2cy00054g.
Szymańska, K., Bryjak, J., Jarzębski, A.B., 2009. Immobilization of invertase on mesoporous silicas to obtain hyper active biocatalysts. Top. Catal. 52, 1030–1036. https://doi.org/10.1007/s11244-009-9261-x.
Szymańska, K., Bryjak, J., Mrowiec-Białoń, J., Jarzebski, A.B., 2007. Application and properties of siliceous mesostructured cellular foams as enzymes carriers to obtain efficient biocatalysts. Microporous Mesoporous Mater. 99, 167–175. https://doi.org/10.1016/j.micromeso.2006.08.035.
Szymańska, K., Ciemięga, A., Maresz, K., Pudło, W., Malinowski, J., Mrowiec-Białoń, J., Jarzębski, A.B., 2021. Catalytic Functionalized Structured Monolithic Micro-/Mesoreactors: Engineering, Properties, and Performance in Flow Synthesis: An Overview and Guidelines. Front. Chem. Eng. 3, 1–14. https://doi.org/10.3389/fceng.2021.789102.
Szymańska, K., Pietrowska, M., Kocurek, J., Maresz, K., Koreniuk, A., Mrowiec-Białoń, J., Widłak, P., Magner, E., Jarzebski, A., 2016. Low back-pressure hierarchically structured multichannel microfluidic bioreactors for rapid protein digestion - Proof of concept. Chem. Eng. J. 287, 148–154. https://doi.org/10.1016/j.cej.2015.10.120.
Szymańska, K., Pudło, W., Mrowiec-Białoń, J., Czardybon, A., Kocurek, J., Jarzębski, A. B., 2013. Immobilization of invertase on silica monoliths with hierarchical pore structure to obtain continuous flow enzymatic microreactors of high performance. Microporous Mesoporous Mater. 170, 75–82. https://doi.org/10.1016/j.micromeso.2012.11.037.
Tong, L., Huang, S., Chen, G., Ouyang, G., 2025. Integrating Enzymes with Reticular Frameworks To Govern Biocatalysis. Angew. Chem. - Int. Ed. 64, e202421192. https://doi.org/10.1002/anie.202421192.
Torrelo, G., Van Midden, N., Stloukal, R., Hanefeld, U., 2014. Immobilized hydroxynitrile lyase: a comparative study of recyclability. ChemCatChem 6, 1096–1102. https://doi.org/10.1002/cctc.201300892.
Van Der Helm, M.P., Bracco, P., Busch, H., Szymańska, K., Jarzębski, A.B., Hanefeld, U., 2019. Hydroxynitrile lyases covalently immobilized in continuous flow microreactors. Catal. Sci. Technol. 9, 1189–1200. https://doi.org/10.1039/c8cy02192a.
Vescovi, V., Kopp, W., Guisán, J.M., Giordano, R.L.C., Mendes, A.A., Tardioli, P.W., 2016. Improved catalytic properties of Candida antarctica lipase B multi-attached on tailor-made hydrophobic silica containing octyl and multifunctional amino-glutaraldehyde spacer arms. Process. Biochem. 51, 2055–2066. https://doi.org/10.1016/j.procbio.2016.09.016.
Vieira, C.S.P., Malafaia, D., Cunha, D.R., Leal, J.F., António, J.P.M., Gois, P.M.P., Garcia-Martinez, J., Noël, T., Poliakoff, M., 2025. RESILIENCE by design: ten principles to guide chemistry in a volatile world. Green. Chem. 27, 7742–7747. https://doi.org/10.1039/d5gc90103k.
Wiedner, R., Kothbauer, B., Pavkov-Keller, T., Gruber-Khadjawi, M., Gruber, K., Schwab, H., Steiner, K., 2015. Improving the properties of bacterial r-selective hydroxynitrile lyases for industrial applications. ChemCatChem 7, 325–332. https://doi.org/10.1002/cctc.201402742.
Wöhler, F., Liebig, J., 1837. Ueber die Bildung des Bittermandelöls. Ann. Phys. 22, 1–24. https://doi.org/10.1002/andp.18371170611.
Woodley, J.M., 2020. New frontiers in biocatalysis for sustainable synthesis. Curr. Opin. Green. Sustain. Chem. 21, 22–26. https://doi.org/10.1016/j.cogsc.2019.08.006.
Woodley, J.M., 2025. A perspective on process design and scale-up for biocatalysis. ChemCatChem 00794, 1–6. https://doi.org/10.1002/cctc.202500794.